

Koopman-Hopf Hamilton-Jacobi Reachability and Control

Will Sharpless, Nikhil U. Shinde, Matthew Kim, Yat Tin Chow and Sylvia Herbert

Abstract—The Hopf formula for Hamilton-Jacobi reachability (HJR) analysis has been proposed to solve high-dimensional differential games, producing the set of initial states and corresponding controller required to reach (or avoid) a target despite bounded disturbances. As a space-parallelizable method, the Hopf formula avoids the *curse of dimensionality* that afflicts standard dynamic-programming HJR, but is restricted to linear time-varying systems. To compute reachable sets for high-dimensional nonlinear systems, we pair the Hopf solution with Koopman theory for global linearization. By first lifting a nonlinear system to a linear space and then solving the Hopf formula, approximate reachable sets can be efficiently computed that are much more accurate than local linearizations. Furthermore, we construct a Koopman-Hopf disturbance-rejecting controller, and test its ability to drive a 10-dimensional nonlinear glycolysis model. We find that it significantly out-competes expectation-minimizing and game-theoretic model predictive controllers with the same Koopman linearization in the presence of bounded stochastic disturbance. In summary, we demonstrate a dimension-robust method to approximately solve HJR, allowing novel application to analyze and control high-dimensional, nonlinear systems with disturbance. An open-source toolbox in Julia is introduced for both Hopf and Koopman-Hopf reachability and control.

I. INTRODUCTION

There are several directions for designing safe controllers for autonomy. The technical rigor involved in planning for success while avoiding failure tends to force methods to sacrifice guarantees (e.g., data-driven methods) or feasibility due to over-conservative solutions (e.g. differential inclusions).

Among these approaches, Hamilton-Jacobi reachability (HJR) is well known for being a robust approach to optimal control and safe path planning [1], [2], [3], [4], [5]. This method is usually used to generate the backward reachable set (BRS) of a system: the set of states from which a system with bounded control can reach (or avoid) a target despite bounded disturbances. This analysis also generates a corresponding optimal controller that rejects bounded disturbances. When feasible, it is a powerful tool for autonomous guidance and other stochastic control problems because of its derivation from the theory of differential games [6], [7] which describes how to optimally drive a system to counter antagonistic or stochastic, bounded disturbances [8]. HJR is, however, often not the most practical approach because of its dependency on spatial gradient approximations in a dynamic-programming (DP) scheme which makes it sensitive to the *curse of dimensionality* [1]. If this theory could be extended to higher dimensional systems, engineering efforts in

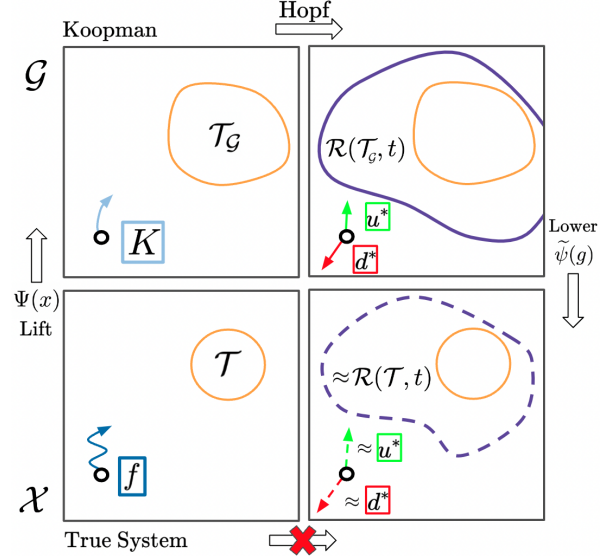


Fig. 1: Graphical Overview The bottom left panel depicts the problem formulation, wherein a system with nonlinear dynamics seeks to either reach or avoid a target set \mathcal{T} . The system may have bounded control and disturbances, formulating a two-player game. The upper-left panel shows the same problem formulation in the lifted linear space, where via Koopman theory the same system is represented by a high-dimensional linear system seeking to reach or avoid the “lifted target” \mathcal{T}_G . The upper-right panel depicts the use of the Hopf solution in this setting to solve the value of the lifted target, yielding the lifted reachable set $\mathcal{R}(\mathcal{T}_G, t)$ and optimal control u^* and disturbance d^* . Finally, the lower-right panel depicts the mapping of the solution to the original space to approximate the true reachable set $\mathcal{R}(\mathcal{T}, t)$ and optimal control and disturbance.

diverse domains, particularly in medicine, finance and other large systems, could make strides where simpler (dimension-robust) controllers are unable to overcome disturbances or model uncertainty.

A. Related Work

Toward this end, several directions have been developed, including set-based propagation, such as the method of zonotopes [9], to over-approximate the Hamilton-Jacobi reachable sets with linear systems [9], [10] and in some special classes of nonlinear systems [11]. The only shortcomings with these methods are that they do not inherently provide an optimal controller and also tend to be overly-conservative.

Another direction is the method of decomposition and system reduction for HJR. The authors of [2] define the system structures that can be decomposed into exponentially-faster, low-dimension problems, however, any coupled dimensions cannot be decomposed. The extension to general systems [12] tends to be overly conservative. There is also a method of projecting coupled systems to independent, lower-dimensional subsystems such that the inverted solution is a

Sharpless, Shinde, Kim, and Herbert are with University of California, San Diego. Chow is with the University of California, Riverside. {wsharpless, nshinde, mak009, sherbert}@ucsd.edu, yattinc@ucr.edu This work is supported by NIH training grant T32 EB009380 (McCulloch) and ONR YIP N00014-22-1-2292. The content is solely the responsibility of the authors.

conjectured over-approximation [13], however, this is often highly conservative and lacks guarantees.

More recently, the Hopf formula was revived [14], [5], [15] as an approach to HJR without sensitivity to dimension or sacrificing guarantees. This method involves interchanging the HJR DP problem for an abstract optimization problem over the characteristic curves of the Lagrange multiplier [14]. This converts the *curse of dimensionality* issue to a *curse of complexity*, because the optimization problem can be non-convex and non-differentiable and requires sophisticated approaches (see [14], [5], [15] for detailed analysis). Nonetheless, certain classes of systems, namely linear time-varying systems, can be robustly solved in both one-player [16], [3] and two-player optimal cases [4], [5]. Notably, in [4] Hopf reachability was paired with a naive linearization method to control a pursuit-evasion nonlinear system with success, although without random disturbance.

We build on the aforementioned strides by novel pairing the Hopf solution with Koopman theory for global linearization. Koopman theory involves “lifting” nonlinear dynamics to high dimensional spaces in order to linearize them with higher accuracy [17], [18]. Multiple works have found that the Koopman procedure can yield highly accurate predictions over a short horizon, suitable for model predictive control (MPC) and linear quadratic regulators (LQR) [19], [20], [21], [22], [23]. Furthermore, we are inspired by recent, impressive work pairing Koopman theory with the method of zonotopes for non-optimal reachability [10].

In this work, we use Koopman theory to define a “lifted” linear reachability problem which approximates our true problem and can be solved by the dimension-insensitive Hopf solution. Note, this sacrifices guarantees, but yields approximations of BRSs and their corresponding optimal controllers for high-dimensional, nonlinear systems for which the only other method is end-to-end learning [24]. A graphical overview of the proposed work can be seen in Figure 1.

B. Contributions and Organization

We make the following contributions:

- 1) We formulate a novel method to approximately solve nonlinear differential games avoiding the *curse of dimensionality*.
- 2) We propose definitions for the corresponding Koopman reachability problem that satisfy the Hopf assumptions, and we compare them in the canonical Koopman problem, the slow manifold system.
- 3) We compare the BRS of our method to that of the DP solution and a Taylor-based solution for both a convex and non-convex game in the Duffing system.
- 4) We synthesize a novel Koopman-Hopf controller and compare it to two Koopman-MPC formulations in a 10-D glycolysis model with bounded, stochastic disturbance.
- 5) We introduce an open-source package *HopfReachability.jl*, for solving 2-player linear differential games.

The paper is structured as follows. Sec. II-A formally introduces HJR, BRSs and the DP solution. Sec. II-B introduces the Hopf solution and its limitations. Sec. II-C introduces Koopman theory to counter these limitations. Sec. III proposes a method of lifting the reachability problem

to the Koopman space that satisfies the Hopf assumptions. Sec. IV demonstrates the Koopman-Hopf method, first, in the Slow Manifold, and second, in the Duffing system where (because of the low dimensionality) its feasible to compare to DP, and third, in a 10D glycolysis system where we compare the novel controller with Koopman-MPCs. Finally, Sec. V summarizes the work and describes future directions.

II. PRELIMINARIES

This paper focuses on control-affine and disturbance-affine systems of the form

$$\dot{x} = f_x(x, t) + h_1(x)u + h_2(x)d \triangleq f(x, u, d, t) \quad (1)$$

where control and disturbance inputs u and d are drawn from convex sets $\mathcal{U} \subset \mathbb{R}^{n_u}$, $\mathcal{D} \subset \mathbb{R}^{n_d}$, and the control and disturbance functions $u(\cdot)$ and $d(\cdot)$ are assumed to be of the set of measurable functions $\mathbb{U} : [t, 0] \mapsto \mathcal{U}$, $\mathbb{D} : [t, 0] \mapsto \mathcal{D}$. Assuming that the dynamics (1) is Lipschitz continuous in (x, u) and continuous in t , there exists a unique trajectory $x(\cdot) \subset \mathcal{X} := \mathbb{R}^{n_x}$ of the system given initial state x , control function $u(\cdot)$, and disturbance function $d(\cdot)$.

A. Hamilton-Jacobi Reachability Problem

To design a safe autonomous controller, HJ reachability solves for the optimal control that counters an adversarial disturbance in a differential game. Here, the control player’s objective is to minimize the game cost while the disturbance player seeks to maximize it [5]. The game is defined by the cost functional

$$P(x, u(\cdot), d(\cdot), t) = J(x(T)) + \int_t^T L(u(\tau), d(\tau))d\tau, \quad (2)$$

where $x(T)$ is the solution of (1) at time T . The terminal cost $J : \mathbb{R}^{n_x} \rightarrow \mathbb{R}$ is a convex, proper, lower semicontinuous function chosen such that

$$\begin{cases} J(x) < 0 & \text{for } x \in \mathcal{T} \setminus \partial\mathcal{T} \\ J(x) = 0 & \text{for } x \in \partial\mathcal{T} \\ J(x) > 0 & \text{for } x \notin \mathcal{T} \end{cases} \quad (3)$$

where $\mathcal{T} \subset \mathcal{X}$ is a user-defined closed set representing the target to reach (or avoid, if the max/min are switched) and $\partial\mathcal{T}$ its boundary. The running cost $L : \mathbb{R}^{n_u} \times \mathbb{R}^{n_d} \rightarrow \mathbb{R}$ serves only to constrain the inputs and, thus, takes the form,

$$L(u, d) = \mathcal{I}_{\mathcal{U}}(u) - \mathcal{I}_{\mathcal{D}}(d) \quad (4)$$

where $\mathcal{I}_{\mathcal{C}}$ are the indicator functions of \mathcal{U} and \mathcal{D} , defined such that

$$\begin{cases} \mathcal{I}_{\mathcal{C}}(c) = 0 & \text{if } c \in \mathcal{C}; \\ \mathcal{I}_{\mathcal{C}}(c) = +\infty & \text{otherwise.} \end{cases} \quad (5)$$

We have now defined the game such that for trajectory $x(\cdot)$ arising from a given x , $u(\cdot) \subset \mathcal{U}$, $d(\cdot) \subset \mathcal{D}$, t , and (1),

$$P(x, u(\cdot), d(\cdot), t) \leq 0 \iff x(T) \in \mathcal{T}. \quad (6)$$

The function $V : \mathbb{R} \times \mathbb{R} \rightarrow \mathbb{R}$ corresponding to the optimal value of the game is defined as

$$V(x, t) = \sup_{d(\cdot) \subset \Gamma(t)} \inf_{u(\cdot) \subset \mathcal{U}} P(x, u(\cdot), d(\cdot), t) \quad (7)$$

where $\Gamma(t)$ is the set of non-anticipative strategies defined in [8], [14], [5], [15] and we assume Isaac's condition [8]. This function is useful because by the same logic of (6),

$$V(x, t) \leq 0 \iff x \in \mathcal{R}(\mathcal{T}, t) \quad (8)$$

where $\mathcal{R}(\mathcal{T}, t)$, the BRS, is the set of all states which can be driven to the target for any bounded disturbance,

$$\mathcal{R}(\mathcal{T}, t) = \{x \mid \exists u(\cdot) \subset \mathcal{U} \forall d(\cdot) \subset \mathcal{D} \text{ s.t.} \\ x(\cdot) \text{ satisfies (1) } \wedge x(T) \in \mathcal{T}\}. \quad (9)$$

Notably, applying Bellman's principle of optimality to this time-varying value function V leads to the following well known theorem.

Theorem 1 (Evans 84). [6] *Given the assumptions (2.1)-(2.5) in [Evan 84], the value function V defined in (7) is the viscosity solution to the following Hamilton-Jacobi Partial Differential Equation,*

$$\frac{\partial V}{\partial t} + H(x, \nabla_x V, t) = 0 \quad \text{on } \mathbb{R}^{n_x} \times [t, T], \quad (10) \\ V(x, T) = J(x(T)) \quad \text{on } \mathbb{R}^{n_x}$$

where the Hamiltonian $H : \mathbb{R}^{n_x} \times \mathbb{R}^{n_x} \times [t, T] \rightarrow \mathbb{R}$ is defined as

$$H(x, p, t) = \min_{u \in \mathcal{U}} \max_{d \in \mathcal{D}} p \cdot f(x, u, d, t). \quad (11)$$

To solve this PDE, therefore, yields the value function and corresponding BRS. Additionally, the value function can be used to derive the optimal control strategy for any point in space and time with:

$$u^*(x, t) = \arg \min_{u \in \mathcal{U}} \nabla_x V(x, t) \cdot g_1(x)u. \quad (12)$$

The main challenge of HJR lies in solving this PDE in (10); DP methods propagate $V(x, t)$ by finite-differences over a grid of points that grows exponentially with respect to n_x [1]. In practice, this is computationally intractable for systems of $n_x \geq 6$ and constrained to offline planning.

B. The Hopf Solution to HJ-PDE's

An alternative to the brute-force grid solving of $V(x, t)$ is the Hopf formula, which offers a solution to (10) in the form of a space-parallelizable optimization problem. First, we define $\phi(x, t) := V(x, T - t)$ to change the aforementioned final-value problem into an initial-value problem for simplicity. ϕ is now the solution of

$$-\frac{\partial \phi}{\partial t} + H(x, \nabla_x \phi, t) = 0 \quad \text{on } \mathbb{R}^{n_x} \times [0, t], \quad (13) \\ \phi(x, 0) = J(x) \quad \text{on } \mathbb{R}^{n_x}$$

with Hamiltonian,

$$H(x, p, t) = \max_{u \in \mathcal{U}} \min_{d \in \mathcal{D}} -p \cdot f(x, u, d, T - t). \quad (14)$$

Note, for systems $f(x, u, d, t) = f(u, d, t)$ without state dependence, the Hamiltonian $H(x, p, t) = H(p, t)$ also lacks state-dependence and in this setting the following Hopf formula is available with limitation. This formula was conjectured in [25], proved to be the viscosity solution in [26] and [7] for $H(p)$, and generalized to some $H(t, p)$ in [27],

[28]. Recently, [14] devised a fast method of solving this formula and [15] conjectured a general form for $H(x, t, p)$.

Theorem 2 (Rublev 2000). *We assume $J(x)$ convex and Lipchitz, and that $H(t, p)$ is pseudoconvex in p and satisfies (B.i-B.iii) in [Rublev 00], then the minimax-viscosity solution [29] of (13) is given by the time-dependent Hopf formula,*

$$\phi(x, t) = - \min_{p \in \mathbb{R}^{n_x}} \left\{ J^*(p) - x \cdot p + \int_0^t H(p, \tau) d\tau \right\} \quad (15)$$

where $J^*(p) : \mathbb{R}^{n_x} \rightarrow \mathbb{R} \cup \{+\infty\}$ is the Fenchel-Legendre transform (i.e. convex-conjugate) of a convex, proper, lower semicontinuous function $J : \mathbb{R}^{n_x} \rightarrow \mathbb{R}$ defined by

$$J^*(p) = \sup_{x \in \mathbb{R}^{n_x}} \{p \cdot x - J(x)\}. \quad (16)$$

Under these assumptions, the minimax-viscosity and viscosity solutions are equivalent when $H(s, p)$ is either convex or concave in p for $s \in [0, t]$ [27], [29].

One may refer to [7], [27], [29], [15] for analysis and comparison of minimax-viscosity and viscosity solutions. Note, only the latter corresponds to the solution of the differential game when the two solutions diverge. If some space-time coupling is permitted, the two solutions may be forced to agree with temporal re-initialization of the value [30], however, this requires caution and we do not attempt it in the current work. For general non-convex H , the question of when these solutions coincide remains open, however, like [15], we observe some agreement in our results.

One may note that there is an alternate form of the Hopf formula, called the Lax formula [25], [7] which swaps the convexity assumption between J and H . This permits a non-convex target but assumes a convex game. Moreover, depending on the method, assuming convexity of both J and H may be required to ensure rapid, global optimization. We discuss these nuances at the end of the section.

The strength of Hopf is that now we may compute (10 & 13) and solve our problem by solving a space-parallelizable optimization problem (i.e. $\phi(x, t)$ does not depend on $\phi(x', t' < t)$), unlike DP [14], [5], [15], avoiding the so called *curse of dimensionality*. However, to require a state-independent Hamiltonian limits this method to a specific class of systems.

It was noted in [28], [14], [5] that any linear time-varying system of the form

$$\dot{x} = A(t)x + B_1(t)u + B_2(t)d \quad (17)$$

can be mapped to a state-independent system

$$\dot{z} = \Phi(t)(B_1(t)u + B_2(t)d) \quad (18)$$

with the linear time-varying mapping $z(t) := \Phi(t; A)x(t)$ defined by the fundamental matrix $\Phi = A(t)\Phi(t)$, $\Phi(0) = I$. If $A(t) \equiv A$, then $\Phi(t; A) = \exp(-tA)$. After the change of variable, the Hamiltonian for ϕ becomes,

$$H_Z(p, t) = \max_{u \in \mathcal{U}} -p \cdot \Phi(T - t)B_1(T - t)u \\ - \max_{d \in \mathcal{D}} -p \cdot \Phi(T - t)B_2(T - t)d. \quad (19)$$

Since the mapping Φ is injective, $\phi_Z(z, t) = \phi(x, t)$ and

$$\phi_Z(z, t) = - \min_{p \in \mathbb{R}^{n_x}} \left\{ J_Z^*(p) - z \cdot p + \int_0^t H_Z(p, \tau) d\tau \right\} \quad (20)$$

where $\phi_{\mathcal{Z}}(z, 0) = J_{\mathcal{Z}}(z(0)) = J(\Phi(T)x(T))$ and we define $T = 0$, thus, $J_{\mathcal{Z}}(z) = J(x)$ and $J_{\mathcal{Z}}^*(p) = J^*(p)$ [5], [3].

Given the convexity of \mathcal{U} and \mathcal{D} , the Hamiltonian in (19) can be rewritten as the difference of two positively homogeneous Hamiltonians given by the convex-conjugates of the indicator functions of \mathcal{U} and \mathcal{D} [5],

$$H_{\mathcal{Z}}(p, t) = \mathcal{I}_{\mathcal{U}}^*(R_1(t)p) - \mathcal{I}_{\mathcal{D}}^*(R_2(t)p), \quad (21)$$

$$R_i(t) := -B_i(T - t)^{\dagger} \Phi(T - t)^{\dagger}.$$

This allows rapid and efficient computation of (20) that has been observed to scale linearly with n_x for a fixed t [5] and demonstrated in online guidance with naive linearizations [4]. Notably, when \mathcal{U} and \mathcal{D} , are constrained by norms, these functions have solutions, namely the dual norms. For example, given $Q \succeq 0$, consider two popular constraints [5], the ellipse and box, and the corresponding \mathcal{I}^* :

$$\begin{aligned} \mathcal{C}_{\mathcal{E}}(Q) &:= \{c \mid \|c\|_{Q^{-1}} \leq 1\} \implies \mathcal{I}_{\mathcal{C}}^*(\cdot) = \|\cdot\|_Q, \\ \mathcal{C}_{\mathcal{R}}(Q) &:= \{c \mid \|Q^{-1}c\|_{\infty} \leq 1\} \implies \mathcal{I}_{\mathcal{C}}^*(\cdot) = \|Q \cdot\|_1. \end{aligned} \quad (22)$$

For these set types, we note the following conditions to certify the convexity of the Hamiltonian (21) for a state-independent system in (18). If \mathcal{U} and \mathcal{D} are defined by the same set type in (22) with Q_u and Q_d respectively, and $B_1 = B_2$, then convexity of the Hamiltonian is given when $Q_u \succeq Q_d$ i.e. when the control authority “exceeds” the disturbance authority. When $B_1 \neq B_2$, convexity of the Hamiltonian is given when $B_1 Q_u B_1^{\dagger} \succeq B_2 Q_d B_2^{\dagger}$ or $[Q_u B_1^{\dagger} \mathbf{1}]_j > [Q_d B_2^{\dagger} \mathbf{1}]_j \forall j$ when the input sets \mathcal{U} or \mathcal{D} are both defined by $\mathcal{C}_{\mathcal{E}}$ or $\mathcal{C}_{\mathcal{R}}$ respectively.

We may note, from the definition of the Fenchel-Legendre (FL) transform, (15) may be rewritten as [7]

$$\phi(x, t) = \left(J^* + \int_0^t H \right)^*(x). \quad (23)$$

This illustrates that the value function is itself an FL transform and from the well known property of the FL transform [7], $\nabla_x \phi(x, t)$ is the minimum argument of (15). Apart from being a perspective for understanding the Hopf solution, we may use this fact to compute the optimal control strategy in (12) immediately from the numerical solution method.

Moreover, we may use this fact for initializing space-neighboring Hopf optimization problems. Considering the well-known Lipschitz continuous quality of ϕ , for $x, x' \in \mathbb{R}^{n_x}$ and p^* and $p^{*'} defined as the corresponding arg min of (15),$

$$\|p^* - p^{*'}\| < \|p^* - 0\| + \|p^{*'} - 0\| < 2L\|x - x'\| \quad (24)$$

Thus, if we are solving independent Hopf problems over a space sequentially, using the minimizing argument of the last problem initializes the optimization within a $2L$ neighborhood of the optimum. In practice, we observe this accelerates convergence by up to 10-fold or greater in high dimensional problems.

Although more scalable than DP (due to the *curse of dimensionality*), the numerical optimization of the Hopf formula is a non-trivial problem discussed at length in [14], [5], [4], [15] (often referred to as the *curse of complexity*). For the examples in this work, we found that the Coordinate-Descent (CD) [31], [32] and the Alternating Direction Method of Multipliers (ADMM) [33], [34] algorithms tailored to the Hopf formula in [5] were suitable for our problems. These

are implemented in our codebase *HopfReachability.jl* and available for public use.

Notably, however, these algorithms impose additional assumptions for solving the Hopf formula: first, for quickly computing the FL transformation (in both CD or ADMM), and second, for computing the proximal mappings (in ADMM). The first condition refers to the need to evaluate J^* in 20 at each iteration, which may require a sub-step optimization if it does not have a closed form (e.g. irregular/piece-wise convex). Recall, that the Hopf formula assumes convexity of J , thus the FL transformation must have a unique optimum but finding this optimum might be slow for high dimensional problems, delaying each iteration of the numerical optimization. Thus, in this work, we limit our problems to targets described by norms, which have closed-form FL transformations (given in 22) [32]. Secondly, if one desires to use ADMM, known to be efficient and dimension-robust [34], one needs to compute the proximal mappings associated with \mathcal{U} and \mathcal{D} at each iteration [5], [15] that also amounts to sub-step optimization. Like before, although we have assumed convexity of each set, irregular convex geometries in high dimensions can slow the convergence to the unique optimum, delaying each iteration of the numerical optimization. Thus, we limit the current work to control and disturbance sets constrained by norms (22).

In summary, the use of the Hopf formula requires several theoretical and practical assumptions that are important to consider. First, we assume J and H convex for the formula to give the value function associated with the game. This requires that our reachability target \mathcal{T} must be convex and the control set \mathcal{U} must exceed the disturbance set \mathcal{D} (22). Second, we assume these convex sets $\mathcal{T}, \mathcal{U}, \mathcal{D}$ are given by norms so that the convergence of the numerical optimization is rapid. These requirements have vital implications for the available lifting functions used in the Koopman methods and the definition of a target in the lifted space.

C. Koopman Theory

Solving a Hopf reachability problem requires access to a linear model representing the system dynamics globally across the state space. Among the options for linearizing nonlinear dynamic systems, Koopman theory is known for outperforming other methods in producing accurate, non-local linearizations [19], [20], [21].

Consider the discretized mapping of a nonlinear system, $x(t_{i+1}) = F(x(t_i))$. The Koopman operator [17], [18] $\mathcal{K} : \mathcal{F} \rightarrow \mathcal{F}$ is defined as $\mathcal{K}g := g \circ F$, where \mathcal{F} is the collection of all functions that form an infinite Hilbert space, often called observables, and $g \in \mathcal{F} : \mathcal{X} \rightarrow \mathbb{R}$ [18], [22]. By definition, the operator has the property,

$$(\mathcal{K}g)(x(t_i)) = g(F(x(t_i))) = g(x(t_{i+1})) \quad (25)$$

and we assume this holds for a finite space such that $\mathcal{K}g \in \mathcal{G}$ [18], [22], where \mathcal{G} is an invariant subspace of the Koopman space. We assume this space is spanned by a finite basis of observables $\{\psi_1(x), \dots, \psi_{n_k}(x)\}$, thus, $K \in \mathbb{R}^{n_k \times n_k}$ is a finite matrix. We call the vector-valued mapping to the concatenated basis $\Psi(x) := [\psi_1(x), \dots, \psi_{n_k}(x)]^{\dagger}$ the lifting function. Then, in practice, for a data set of points $X(t_i)$ and

their one-step evolution $X(t_{i+1})$, K can be approximated from the least-squares problem,

$$\min_K \|\Psi(X(t_{i+1})) - K\Psi(X(t_i))\|^2. \quad (26)$$

Recent works have found this theory can be extended to systems with external inputs [19], [20], [18], [23], [22] such that for $x(t_{i+1}) = F(x(t_i), u(t_i), d(t_i))$. We use the Koopman control form [19], [20],

$$g(x(t_{i+1})) \approx Kg(x(t_i)) + L_1u(t_i) + L_2d(t_i), \quad (27)$$

where L_1 and L_2 are the Koopman control and disturbance matrices. We note that several groups have observed improved accuracy in prediction and control when lifting the inputs (in addition to the state), e.g. with $u_g := \Psi(u)$ or $u_g := \Psi(x, u)$, however, the use of the Hopf formula requires several assumptions that constrain this direction (Sec. II-B), thus, we leave this formulation for future work. The system (27) is similarly fit with control and disturbance data $U(t_i)$ and $D(t_i)$ from a least-squares problem,

$$\min \left\| \Psi(X(t_{i+1})) - \begin{bmatrix} K & L_1 & L_2 \end{bmatrix} \begin{bmatrix} \Psi(X(t_i)) \\ U(t_i) \\ D(t_i) \end{bmatrix} \right\|^2. \quad (28)$$

We note that there are varying technical approaches to solving (26) and (28) and we refer readers to [20], [18], [22], [35] in general, and to [36], [37] for the specific details of the methods used in this work.

Finally, we define a “lowering” function $\tilde{\psi} : \mathcal{G} \rightarrow \mathcal{X}$ for mapping the Koopman predicted evolution in the true space, as in [35], [19], [20], [21], with the only requirement that $\tilde{\psi}(\Psi(x)) \approx x$; this can be a simple projection to the true space when the identity function is included in the lifting dictionary Ψ , as in our examples. Note, the inclusion of the identity function in the lifting function yields theoretical inconsistencies when the system has multiple fixed points, with respect to topological conjugacy [38], [39], or when the system includes linearly-injected control, with respect to the chain-rule [38], [40]. Nonetheless, often accuracy is sufficient within a large region of interest and by nature, allow simple interpretation of the Koopman space, and we include this possibility in our work.

Notably, this lowering function is not injective; due to the approximate nature of (27) (e.g. arising from truncation error, fitting error or control error),

$$K\Psi(x) + L_1u + L_2d \in \mathcal{G} = \text{Span}(\Psi), \quad \text{but} \quad (29)$$

$$K\Psi(x) + L_1u + L_2d \notin \text{Image}(\Psi), \quad (30)$$

where $\text{Span}(\Psi) := \{g | g = c \cdot \Psi(x), c \in \mathbb{R}^{n_k}\} (= \mathcal{G})$, and $\text{Image}(\Psi) := \{g | g = \Psi(x)\}$, the manifold of lifted true states. Hence, trajectories in the approximate Koopman space that start at points lifted from the true space may be driven to points which do not have a correspondence to true points, as discussed in [35]. Yet, we might like to interpret these trajectories and, thus, we allow the lowering function to condense infinitely many Koopman trajectories into the same true trajectory, like in [19], [39], [20], [21]. Although possible, the lowering function is not used in the fitting, however, it guides the definition of a target in the Koopman space in Sec. III that accounts for the

trajectories in discussion, which proved the most accurate for approximating the true reachable set.

III. KOOPMAN-HOPF REACHABILITY

We now seek to approximate the value function and BRS (from Sec. II-A) of our differential game by solving the Hopf formula (20) with approximate linear dynamics derived from Koopman methods. We will first show how to define the target set in the Koopman space, which we call the “lifted target” for its relation to the lifting function. We will then discuss the Hopf requirements that this lifted target must satisfy and the lifting functions that are well-suited to generate a satisfactory lifted target. Finally, we describe how to solve the resulting Hopf reachability analysis using the lifted target set and dynamics.

A. Defining the Lifted Target Set

A target \mathcal{T} defined in Sec. II-A can be lifted directly to the Koopman space such that the lifted target $\mathcal{T}_\mathcal{G}$ is defined as the image of the target \mathcal{T} under Ψ :

$$\mathcal{T}_\mathcal{G} := \{g \mid g = \Psi(x), x \in \mathcal{T}\}. \quad (31)$$

However, given that we may not have an exact linearization as described in Sec. II-C, we also propose an augmented lifted target $\tilde{\mathcal{T}}_\mathcal{G}$ as the preimage of the target \mathcal{T} under the lowering function $\tilde{\psi}$:

$$\tilde{\mathcal{T}}_\mathcal{G} := \{g \mid \tilde{\psi}(g) \in \mathcal{T}\}. \quad (32)$$

This captures the Koopman trajectories which might be driven out of the set of the lifted true states, i.e. the image of the states under the lifting function, to states in the Koopman space for which $\nexists x \in \mathcal{X}$ such that $g = \Psi(x)$ (see Sec. II-C). These two sets are visualized in Figure 2.

If the identity function is included in the lifting function s.t. $\Psi(x) := [x, \psi_1(x), \dots]$ and $\tilde{\psi} := \text{Proj}_\mathcal{X}$, the augmented lifted target is given by the linear combination:

$$\tilde{\mathcal{T}}_\mathcal{G} = \{g \in \mathcal{G} \mid g = [1, c] \cdot \Psi(x), x \in \mathcal{T}, c \in \mathbb{R}^{n_k - n_x}\}. \quad (33)$$

This corresponds to the infinite extrusion of the true target and, thus, if the true target is given by (22) with $A \succeq 0$, then

$$\tilde{\mathcal{T}}_{\mathcal{G},c} = \mathcal{C}(\hat{A}), \quad \hat{A} := \begin{bmatrix} A & 0 \\ 0 & 0 \end{bmatrix} \in \mathbb{R}^{M \times M} \quad (34)$$

is an infinite-length cylinder or rectangular prism. In accordance with the true system, it might be prudent to under-approximate the boundless extrusion to allow some evolution from the lifted true states but limit grandly “abstract” flows, potentially the result of poor Koopman approximation. Moreover, in practice we also find that relaxations of the infinite set, given by defined by $\mathcal{C}(\text{Diag}[A, \varepsilon I])$ for $\varepsilon \gg 1$, accelerate convergence of the Hopf objective (Sec. IV).

B. Conditions for the Lifted Target

The choice of lifting function impacts the shape of the sets $\mathcal{T}_\mathcal{G}$ and $\tilde{\mathcal{T}}_\mathcal{G}$. For the Hopf formula to be a solution to the game, the cost function J and target set \mathcal{T} must be convex¹.

¹One could use the Lax formula to relax this assumption, however, it would ultimately require solving non-convex proximal maps in the numerical optimization.

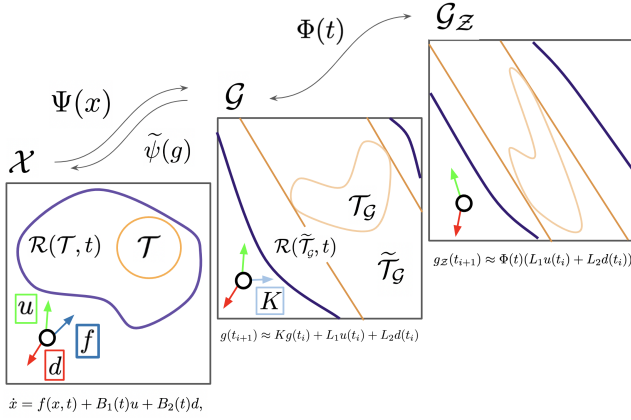


Fig. 2: Sketch of the Involved Spaces & Maps This illustration depicts the three spaces – the space of the true system $\mathcal{X} \subset \mathbb{R}^{n_x}$, the Koopman space $\mathcal{G} \subset \mathbb{R}^{n_k}$, and the state-independent Koopman space $\mathcal{G}_Z \subset \mathbb{R}^{n_k}$ – traversed in this work and the mappings between them: the lifting function $\Psi : \mathcal{X} \rightarrow \mathcal{G}$, the (invertible) fundamental matrix $\Phi : ([0, t], \mathcal{G}) \leftrightarrow \mathcal{G}_Z$, and the lowering function $\psi : \mathcal{G} \rightarrow \mathcal{X}$. This is done to arrive at a space where we can solve the Hopf formula, but requires defining a target (\mathcal{T}_G or $\tilde{\mathcal{T}}_G$) in the “lifted” space that accurately represents the original reachability problem and satisfies the Hopf formula requirements.

Convexity of the lifted target can be enforced by either,

- 1) using a lifting function $\Psi(x)$ that preserves the convexity of a set in the region of the target, or
- 2) using an inner (for reach) or outer (for avoid) convex enclosure, e.g. ball or convex-hull of $\Psi(\mathcal{T})$.

Both methods have nuances worth noting. Using a lifting function that preserves convexity is challenging, given that neither the difference nor concatenation of convex functions generally preserves the convexity of mapped sets. Thus, the notion of a convex basis is ill-defined, and to the best of the authors’ knowledge, there exists no necessary and few sufficient conditions on functions that preserve the convexity of sets. This poses a significant challenge in the certification and construction of specialized lifting functions. Furthermore, we found that lifting functions that preserve convexity generally had greater residual error in the fitting of the Koopman dynamics.

On the other hand, convex-hull methods suffer from the *curse of dimensionality*, but the hull computation is only performed once per problem formulation (for a static reach or avoid target). Note that this method of “convexifying” a lifted target from a non-convex lifting function can be overly conservative for highly non-convex lifting functions. However, this approach is typically preferred, as convex-enclosure methods can be adapted to the broad library of existing lifting functions tried in the literature.

For either case, although the Hopf formula assumes only the convexity of J (and thus \mathcal{T}), to rapidly optimize the objective imposes further conditions regarding convex regularity (Sec. II-B) on a potential lifted target. This regularity is not strictly required to solve the Hopf formula, however, it accelerates the sub-step optimization for online usage.

This paper focuses on convex-enclosures of the lifted target with a norm-constrained set (22) or $\tilde{\mathcal{T}}_G$ which is convex for the true targets given by (22). Ultimately, the method of

convex enclosures was chosen because it is simple to implement and flexible to existing Koopman linearizations. The problems of computing the maximum or minimum bounding ellipse or box are well-known in convex geometry with several available algorithms [41], [42]. Note, although we may use a convex enclosure of the lifted target to over/under approximate the reachable set in the Koopman space (for avoid/reach problems respectively), these are not guaranteed to yield a strict subset/superset of the true reachable set if the Koopman lift of the true dynamics is not exact.

C. Potential Lifting Functions

We demonstrate the proposed method with two simple lifting functions:

- 1) the identity mapping, $I : \mathbb{R}^{n_x} \rightarrow \mathbb{R}^{n_x}$ (i.e. [19])
- 2) the multivariate polynomial of degree l , $P_l : \mathbb{R}^{n_x} \rightarrow \mathbb{R}^M$, $M = \binom{n_x+l}{l} - 1$.

Both cases have been extensively studied in Koopman literature; the former corresponds to dynamic-mode-decomposition with control (DMDc) [19] while the latter is a case of extended-DMD with control [20], [23].

The identity mapping is trivial and thus

$$I(\mathcal{X}) = \mathcal{X} \implies \mathcal{T} = \mathcal{T}_G = \tilde{\mathcal{T}}_G \quad (35)$$

(assuming $\tilde{\psi} = I$). Clearly, our lifted target will be convex if our initial target is convex and computing the FL transform of it will be identical to that of the original target. While this yields a trivial lifted target, it is a fairly limited Koopman method with higher residual error.

The polynomial mapping $P_l(x)$ is more expressive and has been shown to produce more accurate linearizations of dynamics. However, it maps convex sets to non-convex sets, requiring an enclosure to yield a convex lifted target.

Notably, both lifting functions include the identity map. The presence of the identity function in the lifting function makes the definition of the lowering function and the augmented lifted target trivial. However, as discussed earlier, this Koopman system will be inconsistent when used to approximate systems with multiple fixed points and with control [38], [39], [40], ultimately limiting the global quality of the linearization.

D. Conditions for the Lifted Dynamics

In addition to the target convexity, to guarantee that the Hopf formula solves the viscosity solution coinciding with the game - and numerical convergence to the global optimum - convexity of the Hamiltonian is sufficient. If the control and disturbance enter the Koopman space as in (27), the sets will remain convex, however, the (fit) L matrices may alter the relative sizes of the sets such that the Hamiltonian of the Koopman system is not convex.

In the case of reachability problems for systems (1) of the specific form $h_1(x) = h_2(x)$, e.g. when disturbance perturbs control actuation only, we may assume a controlled Koopman system (27) with a corresponding form with $L_1 = L_2$. Then, convexity of the Hamiltonian is given by $Q_u \succeq Q_d$ (see after (22)) which will not be altered in the Koopman fitting process. However, for general Koopman systems where $L_1 \neq L_2$ and they are fit independently, the conditions

$L_1 Q_u L_1^\dagger \succeq L_2 Q_d L_2^\dagger$ or $[Q_u L_1^\dagger \mathbf{1}]_j > [Q_d L_2^\dagger \mathbf{1}]_j \forall j$ must be checked (depending on the set type) to certify convexity of the Hamiltonian. In practice, however, the non-convex Hopf formula (minimax-viscosity solution) can be solved with a powerful optimizer like ADMM and matches the viscosity solution approximately.

Finally, note that if the Koopman system were defined with lifted inputs $u_g := \Psi_u(x, u)$ and $d_g := \Psi_d(x, d)$, the functions Ψ_u and Ψ_d would need to be treated with the same caution as in Sec. III-B to certify the convexity of the Hamiltonian.

E. Koopman-Hopf Procedure Summary

In total, the proposed method involves the following steps, listed in Algorithm 1. First one must choose a lifting function that yields a suitable Koopman system (low residual error in (28)) and lifted target (satisfying Sec. III-B). Next, points of interest – such as a set for interpolating the BRS or a singleton corresponding to an online control program – must be lifted to the Koopman space and then mapped to the state-independent version of it with the fundamental map (and fit K), corresponding to (18). Note, a graphical overview of these involved spaces and mappings can be seen in Fig. 2. Finally, the value at each of these lifted points is solved by optimizing the Hopf formula in (20) and is attributed to the true point that was lifted, approximating the true value. For optimization in this work, ADMM is paired with CD (see *HopfReachability.jl* for parameter details). If interested in the approximate optimal control and disturbance at this point, one may compute these with the minimizing argument (equivalent to the approximate gradient, see (23)) inserted in the relation in (45). If interested in the approximate BRS, one may estimate the zero-level set from the approximate values (e.g. by interpolation).

IV. RESULTS

All results are computed using our codebase *HopfReachability.jl*, an open-source package designed for solving 2-player linear differential games.

A. Approximate BRS of the Slow Manifold

We begin by considering the well-known slow manifold system (see [39], [20] for detailed Koopman analysis),

$$\dot{x} = \begin{bmatrix} \mu x_1 \\ \lambda(x_2 - x_1^2) \end{bmatrix}, \quad (36)$$

with $\mu, \lambda := -0.05, -1$. The autonomous system is famous for being exactly linearizable with the lifting function $\Psi_{SM}(x) := [x_1, x_2, x_1^2]^\top$ such that $g \in \text{Image}(\Psi_{SM}) \subseteq \mathcal{G}$,

$$\dot{g} = \begin{bmatrix} \mu & 0 & 0 \\ 0 & \lambda & -\lambda \\ 0 & 0 & 2\mu \end{bmatrix} g. \quad (37)$$

When (36) has linear control $u \in \mathbb{R}^2$ and disturbance $d \in \mathbb{R}^2$,

$$\dot{x} = \begin{bmatrix} \mu x_1 \\ \lambda(x_2 - x_1^2) \end{bmatrix} + u + d, \quad (38)$$

Algorithm 1 Koopman-Hopf Procedure

Require: For a given system $f(x, u, d)$, \mathcal{U} & \mathcal{D} (1),

Target: $\mathcal{T} \rightarrow J(x)$ (3)

Time(s) to solve: $T - t$

State(s) to solve: X^s (e.g. grid for BRS, one for control)

- 1: Choose $\Psi(x)$ and $\mathcal{T}_G \rightarrow J_G(g)$ satisfying Sec. III-B
 - 2: Fit (K, L_1, L_2) from system trajectories (28)
 - 3: Lift X^s by $\mathcal{G}_Z^s = \Phi(T - t; K)\Psi(X^s)$ (18)
 - 4: **for** $g_Z \in \mathcal{G}_Z^s$ *in parallel* **do**
 - 5: Solve $\phi_Z(g_Z, t)$ by optimization of (20) with J_G^* (16) and H_{G_Z} (19)
 - 6: $V_G(g, T - t), \nabla_{g_Z} \phi_Z(g_Z, t) = \phi_Z(g_Z, t), \hat{p}^*$
 - 7: $\hat{V}(x, T - t) := V_G(g_Z, T - t)$ for $g_Z = \Phi(T - t; K)\Psi(x)$
 - 8: **if** solving strategies **then**
 - 9: $\hat{u}^*(x, T - t), \hat{d}^*(x, T - t)$ are computed with K, L_1, L_2 and $\partial_p H_{G_Z}(\nabla_{g_Z} \phi_Z(g_Z, t), t; \mathcal{U}, \mathcal{D})$ (45)
 - 10: **end if**
 - 11: **end for**
 - 12: **if** solving BRS **then**
 - 13: estimate $\hat{V}(x, T - t) = 0$ for $x \in X$ from $\hat{V}(x, T - t)$ for $x \in X^s$
 - 14: **end if**
 - 15: **return** Approx. BRS $\hat{V}(x, T - t) = 0$ and/or Approx. strategies $\hat{u}^*(x, T - t), \hat{d}^*(x, T - t)$
-

the same lift yields a nonlinear system [39], [23],

$$\dot{g} = \begin{bmatrix} \mu & 0 & 0 \\ 0 & \lambda & -\lambda \\ 0 & 0 & 2\mu \end{bmatrix} g + \begin{bmatrix} 1 & 0 \\ 0 & 1 \\ 2g_1 & 0 \end{bmatrix} (u + d). \quad (39)$$

We may fix g_1 in the control and disturbance matrix, but clearly this yields a local linearization which may be driven off the manifold of true lifted state, given by $g_1^2 = g_3$.

One might question the use of Koopman theory for this application since there exists a local linearization, however, the success of this approach (particularly when coupled with MPC) has significantly outperformed other linearization methods [20], [23], [35]. This motivates the use of these approximate Koopman forms to accommodate trajectories that evolve off the manifold of lifted true states. In the proposed work, omitting the end of these trajectories from the lifted target might omit their origin on the manifold in the backwards-reachable expansion. Hence, we consider four targets in the lifted space and compare their Hopf-solved, BRS evolution for a convex game between control and disturbance.

Consider a reach problem in (38) with a target \mathcal{T} given by a ball of radius $r^x := 1$ centered at $c^x := [0, 1.25]$ and control and disturbance bounded by balls at the origin with radii of $r^u := 0.5$ and $r^d := 0.25$ respectively. We use the approximate Koopman formulation given in (39), defined by lifting function Ψ_{SM} , with $g_1 := 0$ fixed in the input matrix. Following Sec. III, with the image of the true target under the lifting function, \mathcal{T}_G , and pre-image under the lowering function, $\tilde{\mathcal{T}}_G$, we may consider several elliptical targets in the lifted space \mathcal{G} . A 2D slice of these lifted

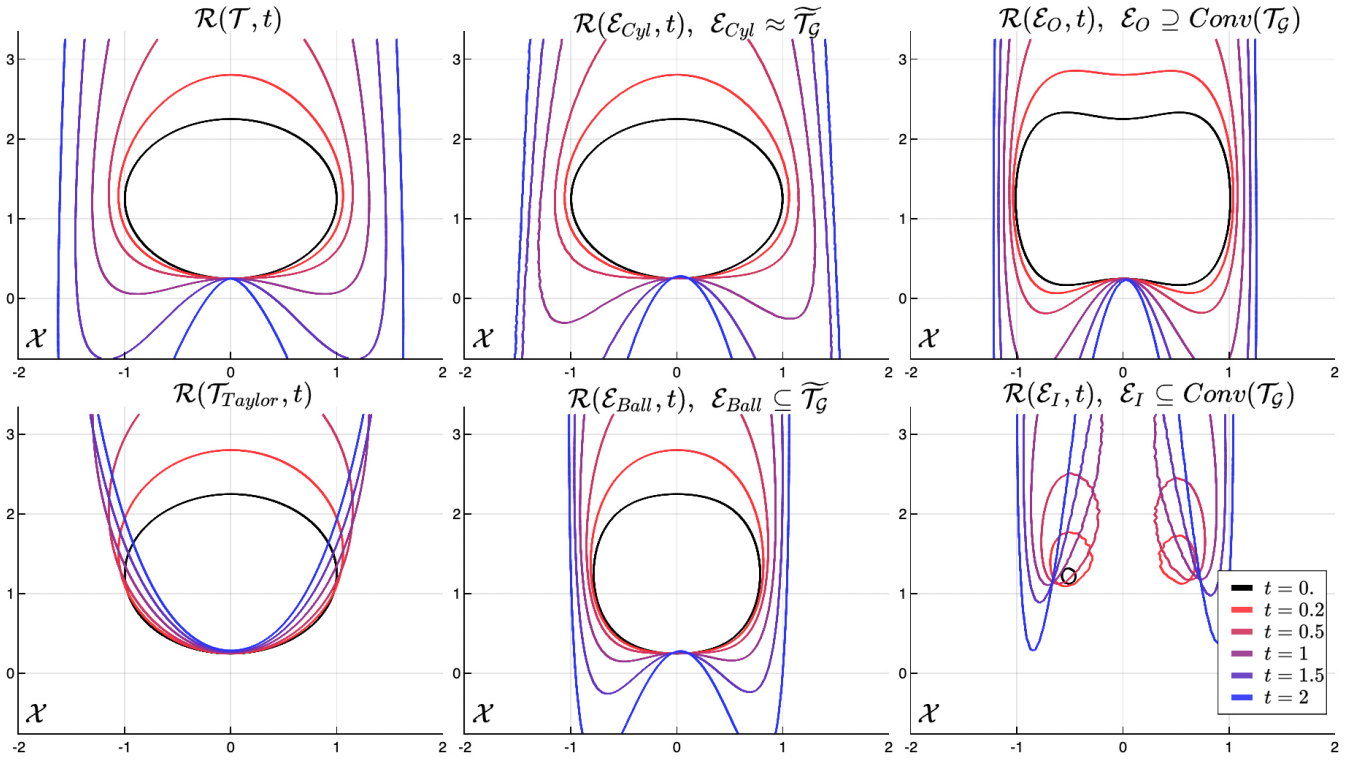


Fig. 3: Koopman-hopf BRS Evolutions for Various Targets in the Slow Manifold System The evolution of the BRS, interpolated as the zero-contour of the Hopf formula over a grid, is plotted for four lifted targets against the DP solution, $\mathcal{R}(\mathcal{T}, t)$ (upper left), and local-linearization Hopf solution, $\mathcal{R}(\mathcal{T}_{Taylor}, t)$ (bottom left), all of which are solved for $t = [0.2, 0.5, 1., 1.5, 2.]$ seconds (spanning red to blue, with the target, i.e $t = 0$, in black). This is done for a convex control and disturbance game in the slow manifold system for which the autonomous dynamics are exactly linearizable, but the control and disturbance dynamics are not.

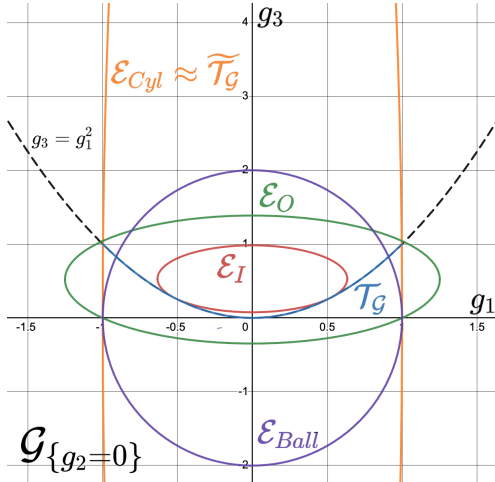


Fig. 4: Lifted Targets for the Slow Manifold This illustration depicts the four targets considered in the $g_2 = 0$ slice of the slow manifold Koopman space \mathcal{G} : the prolate ellipse approximately equal to the augmented lifted target, $\mathcal{E}_{Cyl} \approx \tilde{\mathcal{T}}_G$, the ball, $\mathcal{E}_{Ball} \subseteq \tilde{\mathcal{T}}_G$, the outer ellipse of the lifted target hull, $\mathcal{E}_O \supseteq \text{Conv}(\mathcal{T}_G)$, the inner ellipse of the lifted target hull, $\mathcal{E}_I \subseteq \text{Conv}(\mathcal{T}_G)$.

targets and corresponding reachable sets are visualized in Figure 4. First, we define two targets in the Koopman space based on relaxations (34) of the augmented lifted target $\tilde{\mathcal{T}}_G$: $\mathcal{E}_{Ball} := \mathcal{C}_E(I)$, a ball, and $\mathcal{E}_{Cyl} := \mathcal{C}_E(\text{Diag}[1, 1, \varepsilon])$, a prolate ellipse with $\varepsilon := 15$. Note, the third ellipse axes of these targets, along the lifted state g_3 , are of value greater than zero, hence, $\mathcal{E}_{Ball} \subseteq \tilde{\mathcal{T}}_G$ and $\mathcal{E}_{Cyl} \subseteq \tilde{\mathcal{T}}_G$, and in the

given grid $\mathcal{E}_{Cyl} \approx \tilde{\mathcal{T}}_G$. Second, we define \mathcal{E}_O and \mathcal{E}_I to be the outer and inner ellipses of the convex hull of the lifted target, $\text{Conv}(\mathcal{T}_G)$, solved by semi-definite programs [42]. By definition, these are the unique, minimum-volume enclosing and unique, maximum-volume enclosed ellipses respectively and, hence, $\mathcal{E}_O \supseteq \text{Conv}(\mathcal{T}_G)$ and $\mathcal{E}_I \subseteq \text{Conv}(\mathcal{T}_G)$.

With the procedure Algorithm 1, we plot the BRS evolution for each lifted target on a 100×100 grid in \mathcal{X} lifted to \mathcal{G} . In Figure 3, the top left plot shows the standard HJ DP method using *hj_reachability.py* [43], which is treated as the ground truth. The bottom left plot shows the Hopf formula solved with the Taylor (rather than Koopman) linearization of (38) with the original target \mathcal{T} , called \mathcal{T}_{Taylor} for clarity, linearized at c^x . All other plots show our Koopman-Hopf method with the various target sets (outlined in black). The BRSs at $t = [0., 0.2, 0.5, 1, 1.5, 2]$ look-back times ($T = 0$) are plotted for each lifted target. The contours are solved with the marching squares method using the centripetal Catmull-Rom interpolation scheme [44], [45].

For a quantitative comparison of the results, we compare the $\mathcal{R}(\cdot, t)$ of each result to the DP solution $\mathcal{R}(\mathcal{T}, t)$ with three metrics. The set similarity is quantified by the Jaccard Index [46],

$$JI(\mathcal{R}_1, \mathcal{R}_2) = \frac{|\mathcal{R}_1 \cap \mathcal{R}_2|}{|\mathcal{R}_1 \cup \mathcal{R}_2|}. \quad (40)$$

over the shared grid ($1 \implies$ perfect matching). We also quantify the percentage of False Included and Excluded,

$$\begin{aligned} FI\%(\mathcal{R}_1, \mathcal{R}_2) &= |\mathcal{R}_1 \setminus (\mathcal{R}_1 \cap \mathcal{R}_2)| / |\text{grid}|, \\ FE\%(\mathcal{R}_1, \mathcal{R}_2) &= |\mathcal{R}_2 \setminus (\mathcal{R}_1 \cap \mathcal{R}_2)| / |\text{grid}|. \end{aligned} \quad (41)$$

These measures, along with the average run time per point for each of the approximations, are averaged over $t = [0.2, 0.5, 1.0, 1.5, 2.0]$ and tabulated in Table I.

TABLE I: Mean BRS similarity metrics (best-scoring is bolded) for each of the four lifted targets and the Taylor solution $\mathcal{R}(\mathcal{T}_{Taylor})$ compared to true DP solution, $\mathcal{R}(\mathcal{T})$. Note, the t argument of \mathcal{R} has been dropped to indicate that the results have been averaged over the look-back times $t = [0.2, 0.5, 1.0, 1.5, 2.0]$. The mean comp. time per-point is also given as t_c in milliseconds (ms). Note that each point is computed in parallel.

	$\mathcal{R}(\mathcal{T}_{Taylor})$	$\mathcal{R}(\mathcal{E}_{Cyl})$	$\mathcal{R}(\mathcal{E}_{Ball})$	$\mathcal{R}(\mathcal{E}_O)$	$\mathcal{R}(\mathcal{E}_I)$
JI	0.71	0.94	0.69	0.79	0.17
$FI\%$	0.82	1.18	0.04	4.64	0.00
$FE\%$	17.1	2.3	16.6	7.3	40.7
t_c	3.3	33.0	5.6	5.7	18.5

The BRS plots and Jaccard data demonstrate the best approximation of the true reachable evolution is that of \mathcal{E}_{Cyl} , approximately equal to the augmented lifted target. Thus, many trajectories in this approximate Koopman form beginning at lifted true states must be driven off the manifold under the optimal control and disturbance in a manner akin to true evolution. The drawback of using the cylindrical ellipse is the significant increase in run-time per point, due to parameter ε determining the gradient of the optimization objective, the Hopf formula (20). If speed were the utmost priority and processors limited, a complete BRS analysis might require solving the simpler lifted target \mathcal{E}_{Ball} first to warm-start the solution of \mathcal{E}_{Cyl} .

The inner and outer ellipses may be applied when seeking to minimize the percentage of falsely included or excluded points, respectively. We note, however, these do not provide guaranteed under or over approximations of the true BRS due to the approximate nature of the Koopman dynamics and further work is required to give analytic error bounds.

In summary, we see that the choice of lifted target has a significant implication on the BRS approximation, even for a problem with exactly linearizable autonomous dynamics due to the inclusion of inputs. Nonetheless, the results here demonstrate that the proposed method is viable for approximating the BRS evolution in a manner parallelizable over space which does not scale exponentially with dimension.

B. Approximate BRS of the Duffing Oscillator

Here, we test the Koopman-Hopf approach on the nonlinear Duffing oscillator given by the following dynamics,

$$\begin{bmatrix} \dot{x}_1 \\ \dot{x}_2 \end{bmatrix} = \begin{bmatrix} x_2 \\ \alpha x_1 - \beta x_1^3 - \delta x_2 \end{bmatrix} + \begin{bmatrix} 0 \\ 1 \end{bmatrix} u + B_2 d \quad (42)$$

with $\alpha, \beta, \delta = 1, 1, 0.1$. We consider two problems: the system with disturbance only on the controlled states ($B_2 = B_1$), yielding a convex Hamiltonian, and the system with disturbance on the full state ($B_2 = I$), yielding a non-convex Hamiltonian (see after (22)). In both cases, we consider a target \mathcal{T} defined by a ball with radius of $r = 2$.

To generate an accurate Koopman approximation, we chose to use the 4-degree polynomial $P_4(x)$ (with 15 dimensions) as the lifting-function and fit the Koopman matrices

K , L_1 and L_2 with the hyper-tuning survey performed by *autokoopman.py* package [10], [37]. Given this choice of lifting function containing the identity mapping, the definition of the augmented lifted target $\tilde{\mathcal{T}}_G$ is simply an infinite cylinder with radius $r = 2$, which we relaxed to a prolate ellipse with $\varepsilon = 10$ in the non-identity states of the lift. We solve the BRS evolving from the augmented lifted target with the procedure outlined in Algorithm 1.

We compare our results with an HJR DP method, *hj_reachability.py* [43] as well as the Hopf formula with the true target solved with the Taylor approximation of the system, called \mathcal{T}_{Taylor} . Figure 5 compares the BRSs at $t = [0.66, 1.33, 2]$ look-back times ($T = 0$) for both the convex problem (with disturbance on controlled states only and of less-than or equal magnitude), and non-convex problem (with disturbance on all states).

We quantify the similarity of the sets with the Jaccard Index [46] over a common discretized grid. We additionally include a baseline derived from the Taylor series approximate dynamics with a localization point at the center of the target in \mathcal{X} . The numerical results can be viewed in Table II.

TABLE II: Approximate BRS Jaccard JI similarity to the DP solution, $\mathcal{R}(\mathcal{T}, \cdot)$ for each time in the disturbance on control problem i.e. convex game (left), and disturbance on all states problem i.e. non-convex game (right). Best-scoring is bolded.

t	Convex Game		Non-Convex Game	
	$\mathcal{R}(\mathcal{T}_{Taylor}, \cdot)$	$\mathcal{R}(\tilde{\mathcal{T}}_G, \cdot)$	$\mathcal{R}(\mathcal{T}_{Taylor}, \cdot)$	$\mathcal{R}(\tilde{\mathcal{T}}_G, \cdot)$
0.0	1.0	0.97	1.0	0.97
0.33	0.90	0.96	0.92	0.91
0.66	0.80	0.88	0.85	0.80
0.99	0.61	0.82	0.71	0.66
1.32	0.47	0.78	0.50	0.60
1.65	0.37	0.79	0.37	0.59
1.98	0.30	0.76	0.30	0.58

In Figure 5 and Table II, many important results are apparent. As in the slow manifold system, the Koopman-Hopf method has error that arises immediately from definition of the inexact lifted target, which is not identical to \mathcal{T}_G . Additionally, in the non-convex problem we lose guaranteed convergence to the global optimum of the Hopf formula (the minimax solution) and, separately, agreement between the minimax and viscosity solutions [27], [29], [15], causing further discrepancy between the DP solution and the Taylor and Koopman based Hopf methods in the right columns. In both cases its possible to observe that the Taylor series estimate becomes poor for long horizons while the Koopman-Hopf solution is more robust to error. Particularly in the convex case, its possible to observe that the the Taylor method falls to having only a 30% agreement (by Jaccard), while the Koopman-Hopf method remains above 75% up to $t = 2s$. With improved Koopman and Hopf methods, we expect these results to extend to the analysis and control of more complex, high-dimensional nonlinear systems.

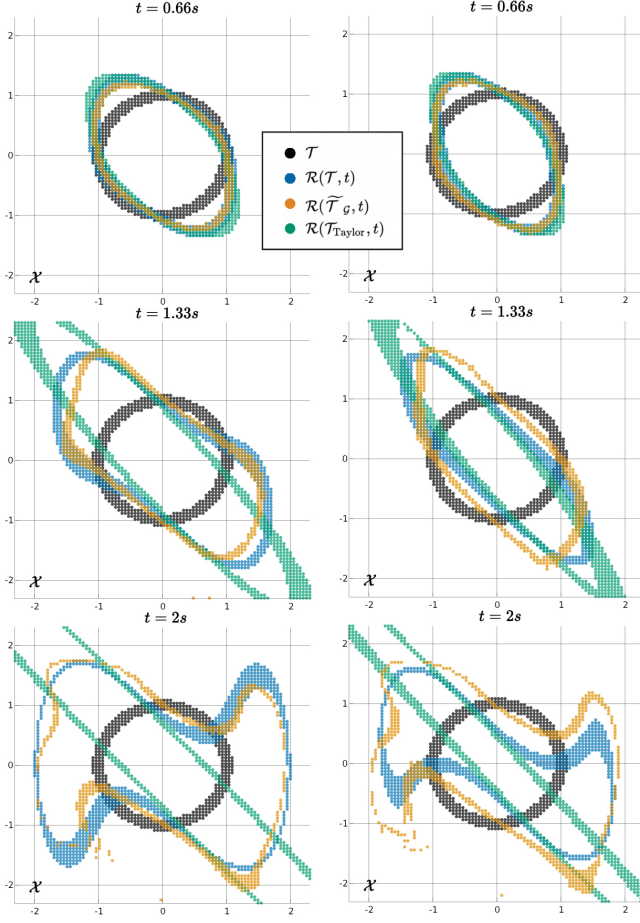


Fig. 5: Koopman-Hopf BRS Evolutions for Convex and Non-Convex Games in the Duffing System Here the $\pm\epsilon$ -boundary ($\epsilon = 0.1$) of a target \mathcal{T} (black), the DP-solved BRS $\mathcal{R}(\mathcal{T}, t)$ (blue), the local-linearization Hopf BRS $\mathcal{R}(\mathcal{T}_{\text{Taylor}}, t)$ (green), and our 15D Koopman-Hopf BRS $\mathcal{R}(\tilde{\mathcal{T}}_g, t)$ (gold) are plotted. In the left column, these correspond to a convex control & disturbance game (disturbance only perturbs controlled states), and in the right column, to a non-convex game (disturbance perturbs all states). Both games are based in the Duffing oscillator and the BRS are plotted for three values of t .

C. Comparison of Koopman control in the Glycolysis Model

Next, we compare the ability of a Koopman-Hopf controller to navigate a 10D glycolysis model [21], [47], [48],

$$\begin{aligned}
 \dot{x}_1 &= \kappa(x_1 - x_7) - \frac{k_1 x_1 x_6}{1 + (x_6/K_1)^4} \\
 \dot{x}_2 &= 2 \frac{k_1 x_1 x_6}{1 + (x_6/K_1)^4} - k_2 x_2 (x_9 - x_5) - k_6 x_2 x_5 \\
 \dot{x}_3 &= k_2 x_2 (x_9 - x_5) - k_3 x_3 (x_{10} - x_6) \\
 \dot{x}_4 &= k_3 x_3 (x_{10} - x_6) - k_4 x_4 x_5 - \kappa(x_4 - x_8) \\
 \dot{x}_5 &= k_2 x_2 (x_9 - x_5) - k_4 x_4 x_5 - k_6 x_2 x_5 \\
 \dot{x}_6 &= -2 \frac{k_1 x_1 x_6}{1 + (x_6/K_1)^4} + 2k_3 x_3 (x_{10} - x_6) - k_5 x_6 \\
 \dot{x}_7 &= u_1 + d_1 \\
 \dot{x}_8 &= \mu \kappa(x_4 - x_8) - k x_8 \\
 \dot{x}_9 &= u_2 + d_2 \\
 \dot{x}_{10} &= u_3 + d_3,
 \end{aligned} \tag{43}$$

where the components of x are [glucose, phosphate pool, 13-BPG, pyruvate/acetaldehyde pool, NADH, ATP, extracellular glucose, extracellular pyruvate/acetaldehyde, NAD+/NADH pool, ATP/ADP pool] and the values of all parameters are inherited from [21]. The model captures the nonlinear enzymatic reaction network for conversion of glucose with cellular currencies ATP and NADH. Note, the dimension of the system makes DP-based HJ optimal control infeasible.

We use the trivial Koopman form corresponding to a 10-dimensional DMDc linearization, which we compute with the *pykoopman.py* package [36]. The Koopman-Hopf controller uses the standard Hopf controller formulation [3], [16], [4] to solve for the minimum time T^* when the target is reachable for the current state x ,

$$T^* = \operatorname{argmin}_T \phi(x, t) = \operatorname{argmin}_T \phi(g, t), \quad g = \Psi(x). \tag{44}$$

The controller then applies the optimal control at this time which is derived from,

$$\nabla_p H(\nabla_{g_z} \phi(g_z, T^*), T^*) = e^{-tK} L_1 u^* + e^{-tK} L_2 d^*. \tag{45}$$

We compare this Koopman-Hopf controller with two Koopman-MPC formulations that incorporate the same Koopman system [49], [20]. The game MPC (MPCg) solves the optimal control for a random fixed disturbance with a one-step horizon, the disturbance then does the same for the previous control, and the process repeats until improvement plateaus. The stochastic MPC (MPCs) [50] samples 20 random disturbance trajectories and minimizes the expectation of the cost given evolution with those samples. In both cases, the MPC algorithms are defined with a horizon of 10 steps of 0.1 seconds (where performance plateaued), and are defined by a terminal cost alone (no running cost) to match the Hopf controller.

All controllers (Hopf and MPC) are based on the same terminal value J which implicitly only defines a target ATP concentration. This encourages the controllers to achieve a specific concentration of ATP, as a bioengineer might desire for cell growth, by manipulating the external glucose, total NAD+/NADH pool, and ADP/ATP pool. This was implemented with another prolate ellipse which is tight only on the ATP dimension, and because of the trivial nature of the lift this target is identical to its lifted forms (35). We chose input sets \mathcal{U} and \mathcal{D} to be ellipses (22) to couple the controls, as common in biological problems, and assume disturbance on actuation only (convex Hamiltonian).

After each controller computes an estimate optimal action $\hat{u}^*(t)$, the system is then progressed with the true nonlinear dynamics (computed with Radau [51]) and a disturbance.

The simulation was run 50 times, with each controller subjected to the same random initial conditions (sampled from the realistic concentration bounds given in [47], [48]) and the same random disturbance trajectory. Results are shown in Table III and Figure 6.

The system is complex because of the highly-stiff nonlinearities, state constraints ($x_i > 0$) and inter-connectivity of the metabolic network; naively driving the ATP/ADP pool up leads to counter-productive results, as demonstrated by MPCg and MPCs in Figure 6.

The Koopman-Hopf controller appears to overcome the nonlinearity of the system by amplifying the oscillations of

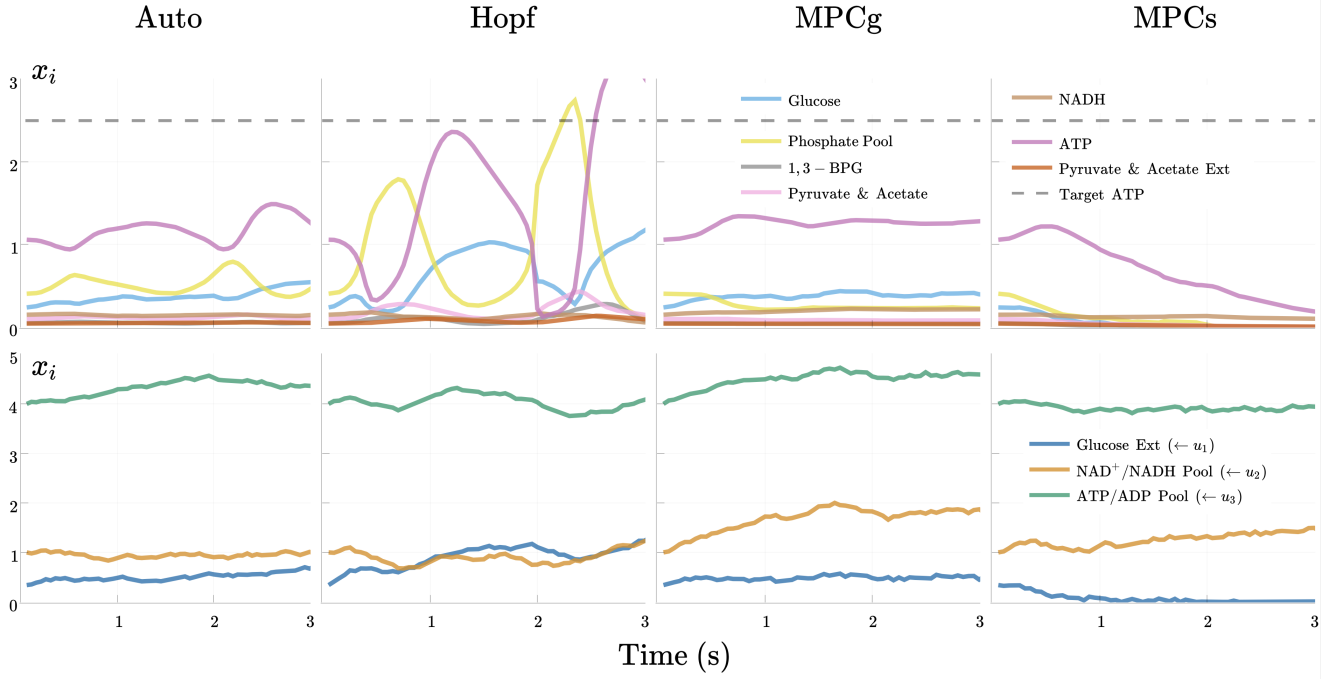


Fig. 6: Comparison of Koopman-based Controllers in a Glycolysis System Three controlled evolutions, using the same Koopman lift, of the 10D glycolysis model with the same disturbance trajectory and initial condition. “Auto” signifies the disturbed autonomous system. The bottom panels plot the three controlled states in the model that can be controlled. Koopman-Hopf controller (“Hopf” above) amplifies the cycle of the phosphate, glucose and ATP states by oscillating the total concentrations of NAD⁺/NADH and ATP/ADP to achieve the target in a manner that translates to the nonlinear system.

TABLE III: Controller Results for 50 random x_0 bounded by [48] and random $d(\cdot)$. The mean comp. time per-point is given as t_c . The best-scoring is bolded.

Controller	Success %	Mean, Max ATP (m)	t_c (s)
Auto	20	2.07	-
Hopf	96	3.06	0.81
MPCg	22	2.14	0.02
MPCs	16	1.96	0.36

ATP to reach the target. From these results, and particularly the failure of the MPCs, navigation to this goal appears to require some long-horizon planning which may be based on a medium-accuracy (linear) model that lacks gratuitous high-resolution fidelity. Furthermore, the observed success is due to the Koopman-Hopf controller’s robustness to disturbance which materialized as model perturbation but also error in the lift. Note, we have no guarantees on the success despite starting in the BRS in the Koopman model. It is also possible be driven to the border of state constraints, despite their implicit effect on the Koopman model generation; to avoid this one would need to cautiously consider the Hopf formula with state constraints [52]. Nonetheless, it is clear from the results that the Koopman-Hopf controller often succeeds despite true disturbance and state constraints. It does this by efficiently computing robust trajectories, unlike the MPC, making the proposed framework a worthy approach for high-dimensional, long-horizon planning.

V. CONCLUSION

We propose a novel Koopman-Hopf method in order to approximate Hamilton-Jacobi reachability in high-dimensional,

nonlinear systems. We find this approach works well for approximating BRSs and driving high-dimensional, nonlinear systems with bounded disturbance. We hope to extend this work along several exciting directions, including expansion to more complicated lifting functions such as radial basis functions and neural networks, applying this to black box systems, and quantifying the uncertainty based on the Koopman linearization error [53]. Moreover, with more advanced methods for Hopf optimization, one might allow a broader class of reachability problems and Koopman methods and we leave this to future work.

ACKNOWLEDGEMENTS

We thank Drs. Steven Brunton, Stanley Bak, Ian Abraham and Masih Haseli for discussions about Koopman theory, Drs. Gary Hower and Matthew Kirchner for discussions about applying Hopf to Naval applications, and Dr. Somil Bansal for thought-provoking feedback. Finally, we thank Zheng Gong and Sander Tonkens for valuable feedback.

REFERENCES

- [1] S. Bansal, M. Chen, S. Herbert, and C. J. Tomlin, “Hamilton-Jacobi reachability: A brief overview and recent advances,” in *2017 IEEE 56th Annual Conference on Decision and Control (CDC)*. IEEE, 2017, pp. 2242–2253.
- [2] M. Chen, S. Herbert, and C. J. Tomlin, “Exact and efficient Hamilton-Jacobi guaranteed safety analysis via system decomposition,” in *2017 IEEE International Conference on Robotics and Automation (ICRA)*. IEEE, 2017, pp. 87–92.
- [3] D. Lee and C. J. Tomlin, “Iterative method using the generalized Hopf formula: Avoiding spatial discretization for computing solutions of Hamilton-Jacobi equations for nonlinear systems,” in *2019 IEEE 58th Conference on Decision and Control (CDC)*. IEEE, 2019, pp. 1486–1493.

- [4] M. R. Kirchner, R. Mar, G. Hower, J. Darbon, S. Osher, and Y. T. Chow, "Time-optimal collaborative guidance using the generalized Hopf formula," *IEEE Control Systems Letters*, vol. 2, no. 2, pp. 201–206, apr 2018. [Online]. Available: <https://doi.org/10.1109/Flcsys.2017.2785357>
- [5] Y. T. Chow, J. Darbon, S. Osher, and W. Yin, "Algorithm for overcoming the curse of dimensionality for time-dependent non-convex hamilton-jacobi equations arising from optimal control and differential games problems," *Journal of Scientific Computing*, vol. 73, pp. 617–643, 2017.
- [6] L. C. Evans and P. E. Souganidis, "Differential games and representation formulas for solutions of Hamilton-Jacobi-isaacs equations," *Indiana University mathematics journal*, vol. 33, no. 5, pp. 773–797, 1984.
- [7] P.-L. Lions and J.-C. Rochet, "Hopf formula and multitime Hamilton-Jacobi equations," *Proceedings of the American Mathematical Society*, vol. 96, no. 1, pp. 79–84, 1986.
- [8] T. Başar and G. J. Olsder, *Dynamic noncooperative game theory*. SIAM, 1998.
- [9] M. Althoff and B. H. Krogh, "Zonotope bundles for the efficient computation of reachable sets," in *2011 50th IEEE conference on decision and control and European control conference*. IEEE, 2011, pp. 6814–6821.
- [10] N. Kochdumper and S. Bak, "Conformant synthesis for Koopman operator linearized control systems," in *2022 IEEE 61st Conference on Decision and Control (CDC)*, 2022, pp. 7327–7332.
- [11] A. Majumdar, R. Vasudevan, M. M. Tobenkin, and R. Tedrake, "Convex optimization of nonlinear feedback controllers via occupation measures," *The International Journal of Robotics Research*, vol. 33, no. 9, pp. 1209–1230, 2014.
- [12] M. Chen, S. L. Herbert, M. S. Vashishtha, S. Bansal, and C. J. Tomlin, "Decomposition of reachable sets and tubes for a class of nonlinear systems," *IEEE Transactions on Automatic Control*, vol. 63, no. 11, pp. 3675–3688, 2018.
- [13] I. M. Mitchell and C. J. Tomlin, "Overapproximating reachable sets by Hamilton-Jacobi projections," 2003.
- [14] J. Darbon and S. Osher, "Algorithms for overcoming the curse of dimensionality for certain hamilton-jacobi equations arising in control theory and elsewhere," *Research in the Mathematical Sciences*, vol. 3, no. 1, p. 19, 2016.
- [15] Y. T. Chow, J. Darbon, S. Osher, and W. Yin, "Algorithm for overcoming the curse of dimensionality for state-dependent Hamilton-Jacobi equations," *Journal of Computational Physics*, vol. 387, pp. 376–409, 2019.
- [16] D. Lee and C. J. Tomlin, "A Hopf-Lax formula in hamilton-jacobi analysis of reach-avoid problems," *IEEE Control Systems Letters*, vol. 5, no. 3, pp. 1055–1060, 2020.
- [17] B. O. Koopman, "Hamiltonian systems and transformation in Hilbert space," *Proceedings of the National Academy of Sciences*, vol. 17, no. 5, pp. 315–318, 1931.
- [18] I. Mezić, "Koopman operator, geometry, and learning of dynamical systems," *Not. Am. Math. Soc.*, vol. 68, no. 7, pp. 1087–1105, 2021.
- [19] J. L. Proctor, S. L. Brunton, and J. N. Kutz, "Dynamic mode decomposition with control," 2014.
- [20] M. Korda and I. Mezić, "Linear predictors for nonlinear dynamical systems: Koopman operator meets model predictive control," *Automatica*, vol. 93, pp. 149–160, 2018.
- [21] E. Yeung, S. Kundu, and N. Hodas, "Learning deep neural network representations for Koopman operators of nonlinear dynamical systems," in *2019 American Control Conference (ACC)*. IEEE, 2019, pp. 4832–4839.
- [22] Y. Li, H. He, J. Wu, D. Katabi, and A. Torralba, "Learning compositional Koopman operators for model-based control," 2020.
- [23] E. Kaiser, J. N. Kutz, and S. L. Brunton, "Data-driven discovery of Koopman eigenfunctions for control," *Machine Learning: Science and Technology*, vol. 2, no. 3, p. 035023, 2021.
- [24] S. Bansal and C. J. Tomlin, "Deepreach: A deep learning approach to high-dimensional reachability," in *2021 IEEE International Conference on Robotics and Automation (ICRA)*. IEEE, 2021, pp. 1817–1824.
- [25] E. Hopf, "Generalized solutions of non-linear equations of first order," *Journal of Mathematics and Mechanics*, vol. 14, no. 6, pp. 951–973, 1965.
- [26] M. Bardi and L. C. Evans, "On hopf's formulas for solutions of hamilton-jacobi equations," *Nonlinear Analysis: Theory, Methods & Applications*, vol. 8, no. 11, pp. 1373–1381, 1984.
- [27] I. Rublev, "Generalized Hopf formulas for the nonautonomous Hamilton-Jacobi equation," *Computational Mathematics and Modeling*, vol. 11, no. 4, pp. 391–400, 2000.
- [28] A. B. Kurzhanski, "Dynamics and control of trajectory tubes. theory and computation," in *2014 20th International Workshop on Beam Dynamics and Optimization (BDO)*. IEEE, 2014, pp. 1–1.
- [29] A. I. Subbotin, "Minimax solutions of first-order partial differential equations," *Russian Mathematical Surveys*, vol. 51, no. 2, p. 283, 1996.
- [30] Q. Wei, "Viscosity solution of the hamilton-jacobi equation by a limiting minimax method," *Nonlinearity*, vol. 27, no. 1, p. 17, 2013.
- [31] J. Bezdek, R. Hathaway, R. Howard, C. Wilson, and M. Windham, "Local convergence analysis of a grouped variable version of coordinate descent," *Journal of Optimization Theory and Applications*, vol. 54, pp. 471–477, 1987.
- [32] S. P. Boyd and L. Vandenbergh, *Convex optimization*. Cambridge university press, 2004.
- [33] D. Gabay and B. Mercier, "A dual algorithm for the solution of nonlinear variational problems via finite element approximation," *Computers & mathematics with applications*, vol. 2, no. 1, pp. 17–40, 1976.
- [34] S. Boyd, N. Parikh, E. Chu, B. Peleato, J. Eckstein et al., "Distributed optimization and statistical learning via the alternating direction method of multipliers," *Foundations and Trends® in Machine Learning*, vol. 3, no. 1, pp. 1–122, 2011.
- [35] D. Bruder, B. Gillespie, C. D. Remy, and R. Vasudevan, "Modeling and control of soft robots using the Koopman operator and model predictive control," *arXiv preprint arXiv:1902.02827*, 2019.
- [36] D. Lab, "pykoopman," 2023, gitHub repository for the pykoopman package. [Online]. Available: <https://github.com/dynamicslab/pykoopman>
- [37] E. J. Lew, "Autokoopman," 2023, gitHub repository for the AutoKoopman package. [Online]. Available: <https://github.com/EthanJamesLew/AutoKoopman>
- [38] Y. Lan and I. Mezić, "Linearization in the large of nonlinear systems and koopman operator spectrum," *Physica D: Nonlinear Phenomena*, vol. 242, no. 1, pp. 42–53, 2013.
- [39] S. L. Brunton, B. W. Brunton, J. L. Proctor, and J. N. Kutz, "Koopman invariant subspaces and finite linear representations of nonlinear dynamical systems for control," *PloS one*, vol. 11, no. 2, p. e0150171, 2016.
- [40] C. Bakker, S. Rosenthal, and K. E. Nowak, "Koopman representations of dynamic systems with control," *arXiv:1908.02233*, 2019.
- [41] F. John, "Extremum problems with inequalities as subsidiary conditions," *Traces and emergence of nonlinear programming*, pp. 197–215, 2014.
- [42] A. Ben-Tal and A. Nemirovski, *Lectures on modern convex optimization*. SIAM, 2001.
- [43] S. ASL, "hj_reachability," 2023, gitHub repository for the hj_reachability package. [Online]. Available: https://github.com/StanfordASL/hj_reachability
- [44] P. T. Inc. (2015) Collaborative data science. Montreal, QC. [Online]. Available: <https://plot.ly>
- [45] P. J. Barry and R. N. Goldman, "A recursive evaluation algorithm for a class of catmull-rom splines," *ACM SIGGRAPH Computer Graphics*, vol. 22, no. 4, pp. 199–204, 1988.
- [46] G. K. Gilbert, "Finley's tornado predictions," *American Meteorological Journal. A Monthly Review of Meteorology and Allied Branches of Study (1884-1896)*, vol. 1, no. 5, p. 166, 1884.
- [47] P. Ruoff, M. K. Christensen, J. Wolf, and R. Heinrich, "Temperature dependency and temperature compensation in a model of yeast glycolytic oscillations," *Biophysical chemistry*, vol. 106, no. 2, pp. 179–192, 2003.
- [48] B. C. Daniels and I. Nemenman, "Efficient inference of parsimonious phenomenological models of cellular dynamics using s-systems and alternating regression," *PloS one*, vol. 10, no. 3, p. e0119821, 2015.
- [49] A. Bemporad, F. Borrelli, M. Morari et al., "Model predictive control based on linear programming: the explicit solution," *IEEE transactions on automatic control*, vol. 47, no. 12, pp. 1974–1985, 2002.
- [50] A. Mesbah, "Stochastic model predictive control: An overview and perspectives for future research," *IEEE Control Systems Magazine*, vol. 36, no. 6, pp. 30–44, 2016.
- [51] E. Hairer and G. Wanner, "Stiff differential equations solved by radau methods," *Journal of Computational and Applied Mathematics*, vol. 111, no. 1–2, pp. 93–111, 1999.
- [52] D. Lee and C. J. Tomlin, "Efficient computation of state-constrained reachability problems using hopf-lax formulae," *IEEE Transactions on Automatic Control*, 2023.
- [53] M. Haseli and J. Cortés, "Temporal forward-backward consistency, not residual error, measures the prediction accuracy of extended dynamic mode decomposition," *IEEE Control Systems Letters*, vol. 7, pp. 649–654, 2022.